

See discussions, stats, and author profiles for this publication at: <https://www.researchgate.net/publication/339937989>

Modelling and optimization of microgrid configuration for green data centres: A metaheuristic approach

Article in *Future Generation Computer Systems* · March 2020

DOI: 10.1016/j.future.2020.03.013

CITATIONS

8

READS

82

3 authors, including:



Rasoul Rahmani

Swinburne University of Technology

57 PUBLICATIONS 1,367 CITATIONS

[SEE PROFILE](#)



I. Moser

Swinburne University of Technology

76 PUBLICATIONS 792 CITATIONS

[SEE PROFILE](#)

Some of the authors of this publication are also working on these related projects:



Interactive optimisation approach to 3D-VRP for the distribution of fibre boards [View project](#)



A hybrid method consisting of GA and SVM for intrusion detection system [View project](#)

Modelling and Optimization of Microgrid Configuration for Green Data Centres: A Metaheuristic Approach

R. Rahmani, I. Moser, A. L. Cricenti

*Faculty of Science, Engineering and Technology, Swinburne University of Technology,
Melbourne, Victoria 3122, Australia*

Abstract

The power load demand of a data centre is in many ways different to that of a residential area. There are differences in the load profiles, the impact of the environmental parameters, the number of peak load demand occurrences in a day as well as peak and off-peak demand. The residential load demand is a complex function of human behaviour which varies based on the geographical, economical, and social characteristics of the consumers. In contrast, estimating the power load of a data centre is rather straightforward. Due to the specific nature of the power load demand of a data centre, finding the optimal configuration of the supplying microgrids can be achieved using off-the-shelf optimisers once an optimisation model has been established. This paper presents a model for finding high-quality microgrid configurations for an enterprise-size green data centres. We present an optimisation model that considers the costs and greenhouse gas emissions associated with all components of the microgrid system, as well as their interactions. The capital, operational, and degradation costs are calculated based on a lifetime of 20 years for the system. Our application of this model to a real scenario of a data centre with a given load demand in a specified environment demonstrates that the model can compose good-quality microgrid configurations for different tradeoffs of cost and sustainability.

Keywords: microgrid design optimisation, green data centre, sustainable computation, metaheuristic optimisation

1. Introduction

Data centre facilities provide businesses with servers, virtual machines, data storage and other services for rent. In 2019, data centres have consumed around 3% of all power generated on the planet [1]. In general, data centres rely on the main power grid for providing the necessary power, which in most countries is still generated using fossil fuels. With the dramatic worldwide growth of the information technology sector, the traffic of data centres and their energy consumption are projected to increase considerably over the coming decades. This will increase the overall cost of running the data centres as well as the greenhouse gas emissions. In this case, one solution that can reduce the power consumption cost is to supply data centres with renewable energy based microgrids, also known as green microgrids [2].

On the other hand, a green microgrid system provides several benefits as an alternative to a conventional electricity infrastructure, especially when the load is concentrated, as it is in a data centre. These include the reduction of transmission losses, increased power generation efficiency, increased reliability, and pollution reduction [3, 4].

Whitfield [1] recently elaborated the importance of green data centres and laid out the opportunities arising from cheaper photovoltaics, which provides the opportunity to self-generate renewable power, which invariably leads to establishing a microgrid for the data centre. This is particularly relevant in the context of Microsoft, Amazon and Google all committing to 100% renewable energy use.

Existing work on green microgrid design discusses mostly two major themes which have to be considered for a successful microgrid architecture: 1. microgrid component selection and sizing and 2. microgrid configuration and operation planning [5, 6, 7].

The first concerns itself with the sizing and selection of components with the objective of minimising capital and operational costs while considering environmental aspects. The selection of the distributed energy resources (DERs), the energy storage system and other components have to satisfy constraints imposed by the power loads, information technology, capital, operational and maintenance costs, climate information, and utility tariff. In addition to the variable nature of renewable energy sources, human behaviour causes load demand fluctuations, which have to be accommodated by the microgrid design methodology [8, 9, 10].

Microgrid operation planning, on the other hand, regulates the optimal

operation in the short/medium term. The aim is to minimise cost while accommodating uncertainty, load fluctuations and unplanned disturbances [11, 12].

Optimising the microgrid system requires considerable computation. Many researchers have focused on developing efficient methodologies that save computations [14, 15]. Several studies have proposed using heuristic optimisation techniques to find near-optimal microgrid configurations. Heuristic techniques have the advantage of converging quicker and escaping from local optima, over most of the mathematical optimisation methods [13, 14].

Radial Movement Optimisation (RMO) is a particle-based optimisation algorithm which has been shown to provide high-quality solutions quicker than other techniques in the categories of Genetic Algorithms (GA) and Particle Swarm optimisation (PSO) [15]. However, any other stochastic optimiser could be used to find good quality results. The main contribution of this work lies in the optimisation model, where the tradeoff between greenhouse gas emissions and cost as part of the objective function is detailed by taking into consideration the degradation of storage and generation units, feed-in tariffs and grid electricity costs as well as defining a cost for emissions. The selection criteria of the renewable energy sources and the parameters affecting the generation of renewables as well as storage are explained and generation and storage units are selected. This contribution is useful in practice, as many smaller data centres decide their proportion of renewable energy based on financial and regulatory considerations [16]. We evaluate the formulation by presenting different variations and their annual costs over a period of 20 years to enable a comparison between microgrid options as well as different assumptions of renewables obtained from the grid.

2. Green Microgrid System Components

The first step in designing a microgrid is the selection of generation and storage components. Since the generation units of a green microgrid are mainly renewables, the local environmental parameters are important for an accurate prediction of the expected power and energy generation. The load demand profile is another key factor in sizing the generation units.

Data centre power loads are less affected by consumer behaviour than residential power consumption. Although consumers cause the demand for the services of data centres, IT load demand is distributed over a wider area.

Therefore, meteorological parameters are more important than demographics, when designing microgrids for data centres. The key components and their parameters are discussed in the following.

2.1. Green data centre load demand

Green data centres are designed, constructed and operated with sustainability as a key criterion [17]. This includes low-emission building materials, sustainable landscaping, and the use of alternative energy technologies such as photovoltaics and wind. Green data centres are designed and constructed for maximal energy efficiency and minimal environmental impact. The microgrids of green data centres also participate in the demand response programs (DR) required by the main power system, managing the data centre's power and communications effectively such that renewable power can be fed to the main grid [18, 19, 20].

Most existing studies focus on modelling and analysing the subsystems of a data centre as independent entities without taking into consideration their interconnections and the influence they have on the energy consumption of other parts of the data centre [21, 22].

The data, air and power flow, as well as the interconnection of all components in a typical green data centre, are shown in Fig. 1, in which the cooling system is assumed to be based on chilled water, the most common design. The data load of a data centre determines its total power consumption. Nevertheless, this relationship is not linear and affected by the heat transfer equations and the power consumption of the electricity supply equipment.

In general, there are three main components for a data centre which are briefly explained in the following.

2.1.1. Information Technology Equipment

Information technology equipment (ITE) consists of a server farm and its power supply which consume about half of the total energy consumed by a typical data centre [23]. This component consists of servers, an uninterruptible power supply (UPS) unit, and power distribution units (PDUs). The computing and storage units of the server farm are placed on racks which contain tens of servers each. A regular data centre facility may be composed of 10,000 racks or about 300,000 servers.

2.1.2. Cooling System

The cooling system is the second most significant power consumer in a data centre. Removing the heat from the servers, it is commonly based on a

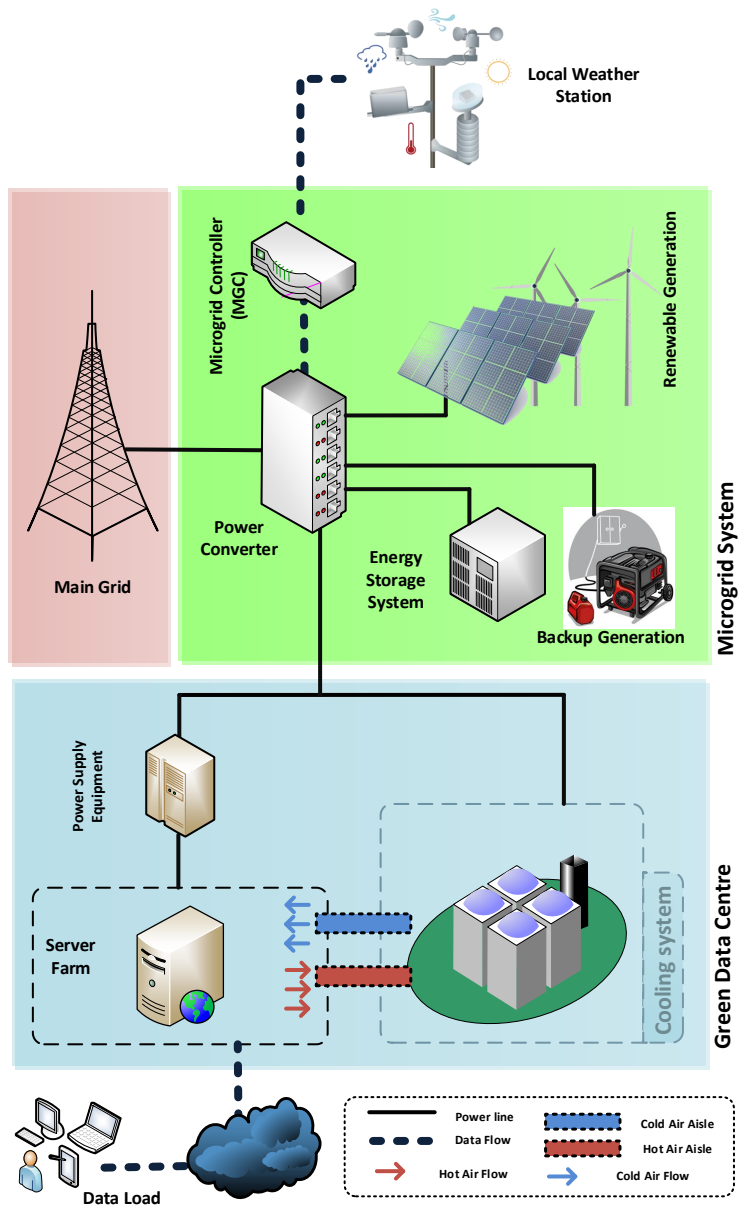


Figure 1: The interactions of green data centre, microgrid, and the main grid.

water chiller plant in which a vapour-compression or absorption cycle is used to reduce the temperature of the cooling fluid. There are different techniques for transferring heat between the data centre and the cooler using transport fluid in data centres [24]. The ambient temperature has a considerable impact on the power consumption of the chiller plant.

2.1.3. Miscellaneous Power Consumption

Lighting, security devices, control and monitoring systems, as well as networking facilities are categorised as miscellaneous power consumption, which is independent of server utilisation or environmental parameters. It is affected only by the size of data centre and makes up approx. 6% of the total power consumption.

2.2. Generation units and energy storage system

The selection of distributed energy resources (DER) for a microgrid requires the consideration of load type and priority, average load and available distributed energy resource technologies [25, 26]. The optimal size of the selected DERs are dictated by considerations of capital cost, installation cost, operation and maintenance cost, power rating, reliability of the system, greenhouse gas emissions, and the lifetime of microgrid. The cost benefit of microgrids based on renewable energy is often calculated by comparing the cost of energy extracted from the DER units with the same amount purchased from the main grid. However, cheap energy is not the sole aim of designing a DER based microgrid system; environmental friendliness and energy security are factors to consider when planning power distribution systems [27].

The power generation system considered in this research includes photovoltaics and wind with a battery system for energy storage. Hydro-power is not included in the mix of renewable energy sources, because it does not lend itself for inclusion as a component. The opportunity for hydro arises in specific environments, whereas microgrids that serve a specific data centres are co-located with the data centre to avoid transmission losses. Due to the large size of hydro stations, unlike in previous centuries, these are now connected to the main grid rather than a microgrid [28].

The power generation of photovoltaic (PV) panels mainly depends on the solar irradiation which can be obtained from Eq. (1) [29].

$$\mathcal{P}_{PV} = \frac{\mathcal{H}}{1000} \times \quad (1)$$

$$\left[\mathcal{P}_{max} + \mu_{\mathcal{P}_{max}} \left(\mathcal{T}_{amb} + \mathcal{H} \frac{NOCT - 20}{800} - 25 \right) \right]$$

where \mathcal{H} is the solar irradiation in W/m^2 , \mathcal{P}_{max} is the peak power being generated by the PV panel, $\mu_{\mathcal{P}_{max}}$ denotes the temperature coefficient of the maximum power point, \mathcal{T}_{amb} is the ambient temperature of the PV panel, and $NOCT$ denotes the normal operating cell temperature of the PV panel. The 25 denotes the standard ambient temperature in Celsius, while other constants are 800 as global solar flux in W/m^2 , and 20 as air temperature in Celsius, measured in the nominal terrestrial environment (NTE) and reported by Stultz and Wen [30].

The power generation model used for the wind turbines is shown in Eq. (2). Each wind turbine's rated power is 100 kW; therefore, the optimal size of the wind energy system is to find the optimal number of wind turbines. It is worth mentioning that the wake effect in a wind farm is neglected in this study [31].

$$\mathcal{P}_{WT} = \beta_1 \times \mathcal{V}^2 + \beta_2 \times \mathcal{V} \quad (2)$$

where $4 \leq \mathcal{V} \leq 25$ is the wind speed in m/s , and \mathcal{P}_{WT} is equal to zero for other values of the wind speed due to cut in and cut off constraints of the wind turbine. The β_1 and β_2 constants are based on the wind turbine characteristics which are equal to 1.43 and -4.29, in this study.

In energy management systems, the mathematical model of the battery system includes the state of charge (SOC) and charging/discharging rate (C-rate) [29] while detailed battery model consisting of a set of partial differential equations (PDE) for the voltage level and its associated constraints as presented by Zou *et al.* [32], is neglected. While the charge and discharge time vs. C-rate depend on the battery type, in general, a higher C-rate leads to faster charge and discharge for the battery energy stored [33]. A high C-rate degrades the battery lifetime and efficiency. Regarding the SOC of the battery system, some constraints have to be taken into account. As suggested by Prajapati *et al.* [34], a SOC greater than 20% can help bridge the gap between the renewable energy shortage and the load demand. On the other hand, overcharging of the battery to more than 80% of SOC is not recommended due to possible physical damages to the storage system.

The energy storage system has been mainly used to enhance the stability and efficiency of the microgrid system. It provides the possibility of reducing the peak generation value as well as adapting the generation with consumer's time of use pattern by performing power balancing between the load demand

and energy generation [35, 36].

3. Microgrid Optimisation Model

This section provides mathematical models for the costs and the greenhouse gas emissions associated with all components of the microgrid system, in order to optimise the size of renewable generation units and the storage system using hourly simulation of electricity power, costs, and emissions.

Each arbitrary sizing of the microgrid is evaluated based on the summation of hourly operational costs and an equivalent present-time cost for their capital and lifetime costs, as well as the greenhouse gas emissions. The evaluation is performed using a fitness function composed of the associated costs and emissions. For a given configuration, the output power of each renewable generation unit and the load demand are calculated based on the local environmental parameters.

Ultimately, the optimal size of the microgrid components for the given green data centre will have the minimum annual fitness value. The optimisation algorithm and the fitness function are presented in Section 4. The technical aspects of the microgrid topologies such as AC or DC are not within the scope of this research work.

3.1. Generation and storage costs

Photovoltaic generation generally does not incur much operational cost, but its capital cost is quite considerable. Both maintenance and operational cost of wind turbines and the capital investment cost are high. In this study, the fixed annual cost (C_{an}^{fix}) of PV and wind energy are set to 650 and 480 \$/kWyear, as used by Mizani and Yazdani [37]. Since some utility companies agree to buy the excess renewable energy generation using a feed-in tariff, this has to be considered in the model as a feed-in rate (\mathcal{R}) which normally varies based on the utility companies and also the type of renewable energy system. The feed-in rate is usually quite small compared to the retail price of the electricity, and was set to 0.14 \$/kWh for both PV and wind energy, in this study. Eq. (3) shows the annual cost C_{an} for g^{th} renewable energy generation units.

$$C_{an}[g] = C_{an}^{fix}[g] - \sum_{h=1}^{8760} \mathcal{P}_g[h] \times \mathcal{R}_g \quad (3)$$

where $\mathcal{P}_g[h]$ is the power sold to the utility company at h hour from g^{th} renewable energy generation unit, here assuming a year (8760 hours).

For the battery system, in addition to a fixed installation and investment cost, degradation cost (\mathcal{D}) has to be considered. Although the exact degradation cost of a battery system can be dependent on the depth of discharge (DOC) and SOC, it is accurate enough to assume it as a fixed cost per kW. The total annual cost of the battery system consists of a fixed annual cost ($C_{an}^{fix,bat}$) representing the investment and installation costs, and the charge/discharge degradation cost which is calculated by multiplying the charge/discharge power (\mathcal{P}_{bat}) by the degradation rate (\mathcal{D}). The annual cost of the battery system is obtained using Eq. (4).

$$C_{an}^{bat} = C_{an}^{fix,bat} + \sum_{h=1}^{8760} \mathcal{P}_{bat}[h] \times \mathcal{D} \quad (4)$$

In this study, the ($C_{an}^{fix,bat}$) is 240 \$/kW $year$ and the degradation rate (\mathcal{D}) is 0.04 \$/kW.

In addition, the total annual cost for generation and storage is then calculated as shown in Eq. (5), where $C_{an}[g]$ represents the annual cost of the g^{th} generation unit and \mathcal{N}_{RE} denotes the total number of renewable energy generation units.

$$C_{an}^{total} = \sum_{g=1}^{\mathcal{N}_{RE}} C_{an}[g] + C_{an}^{bat} \quad (5)$$

3.2. Grid electricity costs

The electricity purchased from the utility companies is considered as purchased from the grid which can be represented by various cost functions relative to the tariff ($f_{grid}(\mathcal{P}_{grid})$). Therefore, the annual cost of the electricity purchased from the grid can be obtained from Eq. (6).

$$C_{an}^{grid} = \sum_{h=1}^{8760} f_{grid}(\mathcal{P}_{grid}[h]) \quad (6)$$

where \mathcal{P}_{grid} is the hourly power purchased from the grid in kW. In this study, the price function of the grid electricity is considered to be flat rate at 0.26 \$/kWh.

Table 1: Emission factors for different green gas pollutants

pollutant	CO_2	CO	UHC	SO_2	NO_x	PM
\mathcal{X}_p	0.632	6.5e-3	7.2e-4	7.2e-4	1.34e-3	4.9e-4

3.3. Emissions costs

The greenhouse gas emissions are another factor in microgrid design and planning which is modelled as a cost in this study. No pollutant is taken into account for PV, wind generation and battery system, but the total annual emissions (E_{an}) of the electricity purchased from the grid is obtained using Eq. (7).

$$E_{an} = \sum_{h=1}^{8760} \mathcal{P}_{grid}[h] \times \sum_{p=1}^{\mathcal{M}} \mathcal{X}_p \quad (7)$$

where \mathcal{M} is the number of pollutants and \mathcal{X}_p is the emission factor of p^{th} pollutant in kg/kWh . The major pollutants considered in this study are Carbon Monoxide (CO), Carbon Dioxide (CO_2), Sulfur Dioxide (SO_2), Unburnt Hydrocarbons (UHC), Particulate Matter (PM), and Nitrogen Oxides (NO_x) which are represented with their emission factors in Table 1 [37]. Since the emission factors depend on the fuel mix burnt in the power plants, their real values might vary between two power systems. Therefore, the presented values are rough assumptions for a power system relying on coal fired power plants. For instance, if the majority of the grid electricity is generated by the nuclear power plants, the grid emission factors are lower than what presented in Table 1. The unit for the pollutant emission factor is kg/kWh that results in kg being the unit for the total annual emissions.

3.4. Microgrid Power Balance

There are two factors for consideration in microgrid reliability which are loss of power supply (LPS) and loss of load (LOL) [29]. In this study, the prime power suppliers for the load demand of the green data centre (\mathcal{P}_{GDC}) are solar power (\mathcal{P}_{PV}^{tot}) and wind power (\mathcal{P}_{WT}^{tot}). If the load demand \mathcal{P}_{GDC} is greater than the total renewable power generation ($\mathcal{P}_{PV}^{tot} + \mathcal{P}_{WT}^{tot}$), there are two options to supply the excess load: battery power \mathcal{P}_{bat} , and purchasing from the grid \mathcal{P}_{grid} . In case that there is excess renewable generation $\mathcal{P}_{PV}^{tot} + \mathcal{P}_{WT}^{tot} > \mathcal{P}_{GDC}$, the battery will be charged first, the remaining power will be fed into

the main grid. Therefore, battery power and the grid power are used to ensure that the power balance shown in Eq. (8) must always hold.

$$\mathcal{P}_{PV}^{tot} + \mathcal{P}_{WT}^{tot} + \mathcal{P}_{grid} = \mathcal{P}_{GDC} + \mathcal{P}_{bat} \quad (8)$$

4. Radial movement optimisation

Radial Movement Optimization (RMO) [38] is a metaheuristic global optimisation algorithm that uses a vectorised search space to model the problem environment where each particle at each step proposes a solution to the problem and the overall movement of the particles is towards better areas of the search space. RMO is initialised according to Eq. 9.

$$X_{i,j} = X_{min(j)} + rand(0,1) \times (X_{max(j)} - X_{min(j)}) \quad (9)$$

where $X_{i,j}$ is the location matrix of the particles, i represents the number of particles and j the number of dimensions. $X_{min(j)}$ and $X_{max(j)}$ represent the constraints for the j^{th} dimension. $rand(0,1)$ is drawn from a normal distribution.

The centre point cp is the location of the particle with the best fitness value, obtained after the initialisation.

The velocity matrix $V_{i,j}$ determines how far each particle moves. The inertia weight W_k (Eq. 10) is updated after each generation to determine the convergence rate of the algorithm.

$$W_k = W_{max} - \left(\frac{W_{max} - W_{min}}{it_{max}} \right) \times it_k \quad (10)$$

$$V_{i,j}^k = W_k \times rand(0,1) \times V_{max(j)}$$

Since the velocity matrix is dependent on the inertia weight, the values of W_{max} and W_{min} determine the convergence strategy. In this study, they are set to 1 and 0.2 respectively based on preliminary investigations.

The location of the best fitness value is stored as the radial best ($Rbest$). The best $Rbest$ of all past iterations is the global best ($Gbest$). The vector diagram of the particle movement is shown in Fig. 4.

The location of the $Rbest$ and $Gbest$ are used to create the update vector up , which is obtained by Eq. (11) and used to update the location of cp for

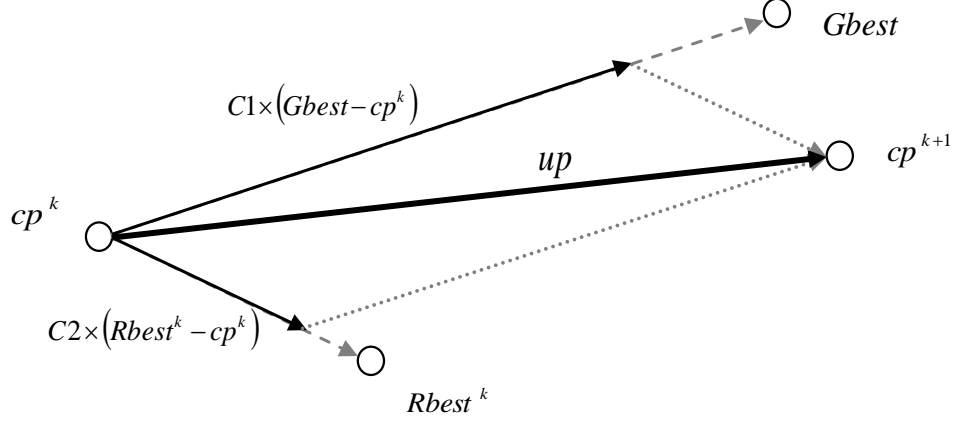


Figure 2: How to update the centroid.

the next iteration, as shown in Eq. (12).

$$cp^{k+1} = cp^k + up \quad (11)$$

$$up = C1 \times (Gbest - cp^k) + C2 \times (Rbest - cp^k) \quad (12)$$

In Eq. (12), $C1$ and $C2$ are the movement coefficients and must be set by the user. The process is repeated for the set number of iterations, where the particles' positions will be determined based on new centroids cp .

The stopping criterion can be either a maximum number of iteration or a minimum value of deviation for the $Gbest$; i. e. the α value being smaller than a predefined number in Eq. (13).

$$\alpha = |G_{best}^{new} - G_{best}^{old}| \quad (13)$$

For a detailed description of the algorithm see Rahmani and Yusof [38].

4.1. Search space and fitness function

For RMO to find good solutions to a problem, the multidimensional solution space which contains all possible solutions has to be defined. In this study, the search space consists of \mathcal{N}_{PV} , \mathcal{N}_{WT} and \mathcal{N}_{bat} which are the numbers for PV panels, wind turbines and battery banks respectively. Each 20 PV modules of 250 W (i.e. 5 kW) is considered to be the minimum scale for installation. In general, the configuration that proposes the lowest cost and

emissions is desired; however, there is always a trade-off between these two parameters. Hence, the optimisation problem and its constraints become as stated in Eq. (14).

$$\begin{aligned}
& \min (\theta \cdot C_{an}^{total} + (1 - \theta) \cdot E_{an}) & (14) \\
& \text{subject to: } \mathcal{N}_{PV} = 20 \times x_1 : x_1 \in \mathcal{Z}^* \\
& \quad \mathcal{N}_{WT} = x_2 : x_2 \in \mathcal{Z}^* \\
& \quad \mathcal{N}_{bat} = x_3 : x_3 \in \mathcal{Z}^* \\
& \quad 0 \leq \theta \leq 1
\end{aligned}$$

where the θ value denotes the trade-off factor between the cost and emissions.

5. Simulation Results and Discussion

In this section, we present the power load demand based on real climate data and the microgrid design optimisation results.

5.1. Environmental parameters

In this study, the hourly environment temperature, irradiation, and wind speed are obtained from the National Renewable Energy Laboratory (NREL) website [25]. Fig. 3 shows the hourly temperature profile for the first week of June 2016 (summer week) and December 2016 (winter week). In addition, the hourly solar irradiation and wind speed for a summer week is shown in Fig. 4.

5.2. Data centre load demand simulation

As a case study for modelling, we assume a data centre with a structure shown in Fig. 1 and a server farm consisting of 40,000 computer servers. The annual hourly server utilisation and power consumption of the data centre are generated based on the weekly utilisation profile presented by Macías and Guitart [39] and the simulation power model presented in [40]. Fig. 5 shows the annual hourly power consumption profile of the data centre for whose microgrid configuration is optimised.

The statistical analysis of the power load, presented in Table 2, shows that the power consumption is never less than 60% of the average power

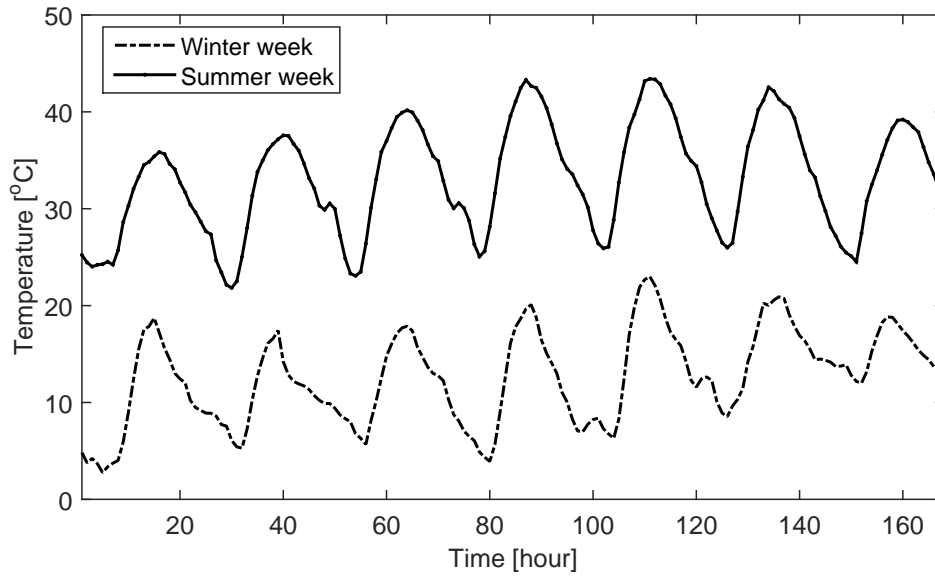


Figure 3: Hourly outdoor ambient temperature of data centre for one week.

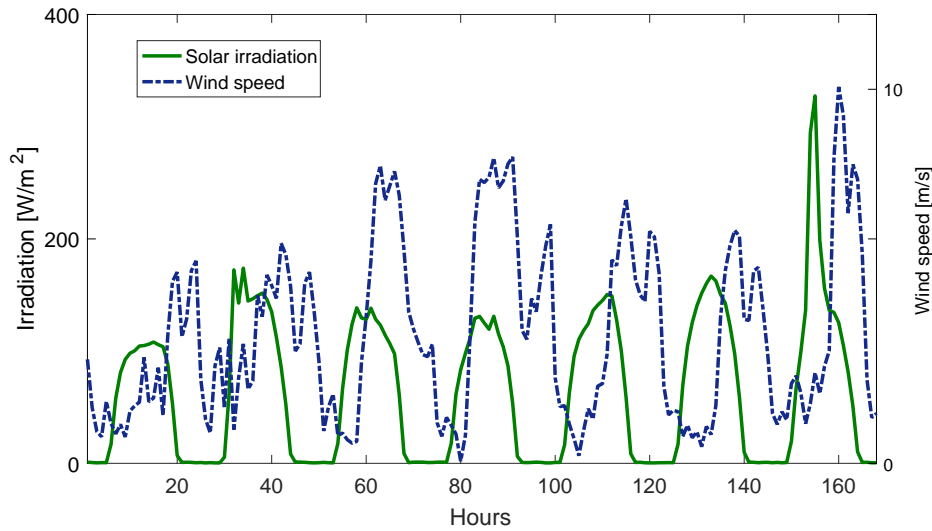


Figure 4: Hourly outdoor ambient temperature of data centre for one week.

consumption which means the data centre always requires a huge amount of power, even at its off-peak times. Also, the total annual energy consumption of the data centre is about 118.7 GWh.

Table 2: Statistical analysis of the annual power consumption profile of the data centre.

Min.	Max.	Mean	Median	Stdev	Range
8.1e+06	2.3e+07	1.4e+07	1.3e+07	3.6e+06	1.5e+07

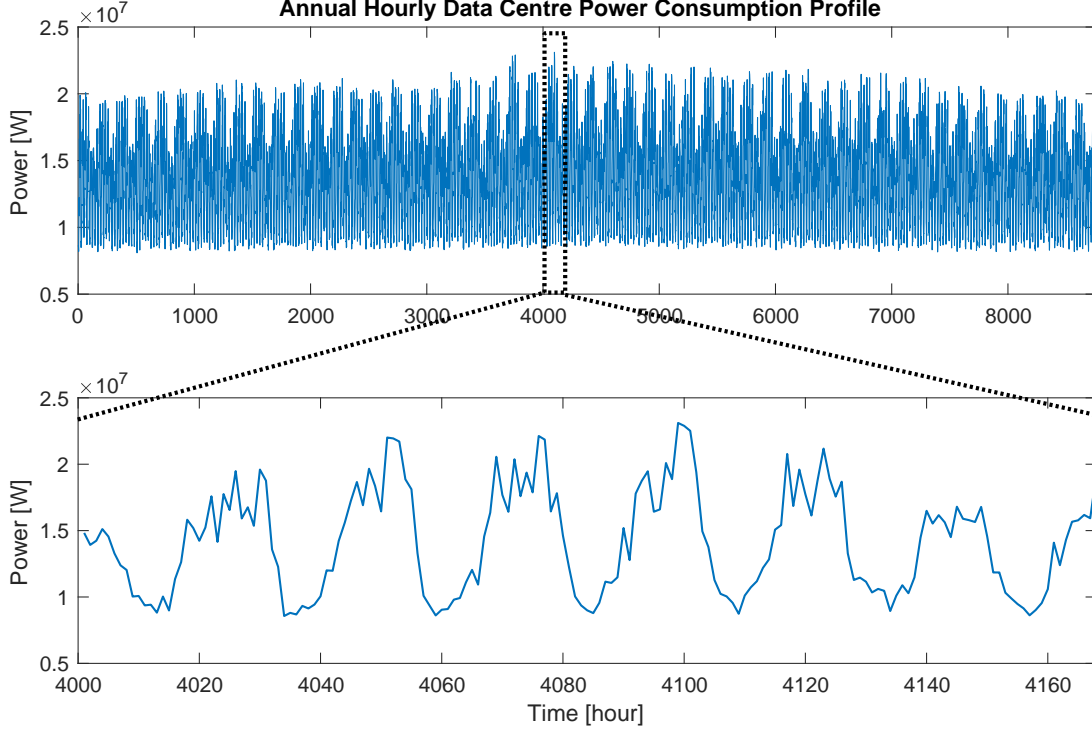


Figure 5: Generated annual hourly power consumption profile of the data centre.

5.3. Microgrid design optimisation

Based on the annual hourly data and the models for renewable energy generation units and battery system, the a near-optimal configuration of the microgrid is obtained using RMO. The number of particles is set to 10 and the stopping criterion is either reaching the maximum iteration of 200 or the α value in Eq. (13) be less than 10^5 . The experiment included 10 simulation runs, whose results were identical. Each run takes less than 10 minutes. As the base scenario, the trade-off factor between the cost and emissions was set to 0.7. Further analysis on the impact of this factor on the resulting configuration is presented in Section 8.

Table 3 shows the capacity of PV, wind and battery systems and some details about the cost and emission for the configuration obtained from the optimiser as well as the grid-only solution. The annual 24-hour moving average of the data centre load and the total renewable power generation of the optimised configuration is demonstrated in Fig. 6.

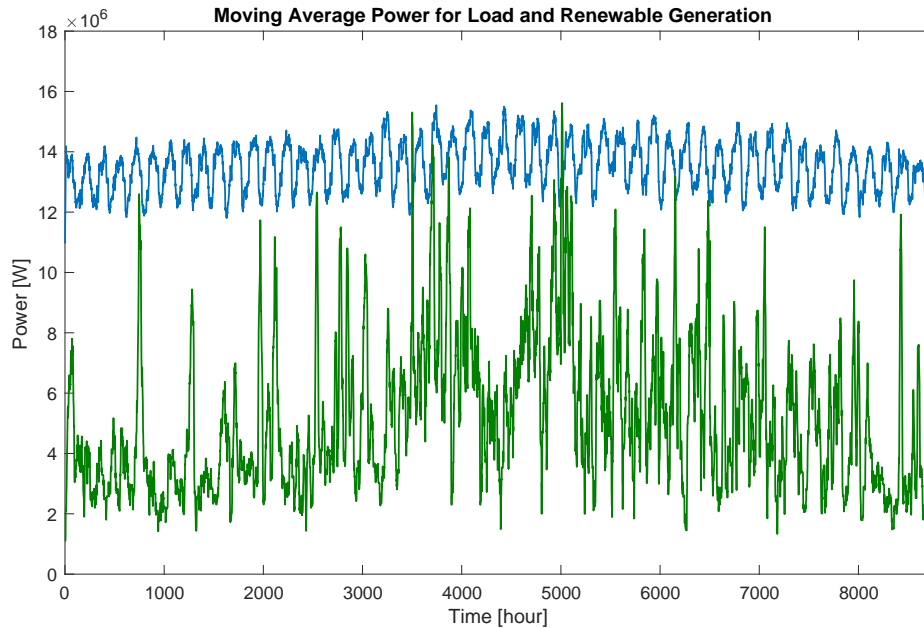


Figure 6: 24-hour moving average of the data centre load and the total renewable power generation during one year for the base scenario.

Fig. 7 shows the annual contribution of different energy sources in supplying the electricity of the green data centre. It can be observed that the renewable sources supply 38% of the load demand for a year while wind energy provides 6% more than that of PV systems with 16%. The main grid still provides 62% of the electricity required for the data centre.

The energy control and management strategy is based on supplying the load demand with the renewable energy generation and storing the excess green energy generation in the batteries. In case that the batteries are charged fully, the power can be fed into the grid. If the renewable energy is insufficient, first, the batteries will be discharged to supply the load demand, and in the second instance, power will be purchased from the grid. Fig. 8

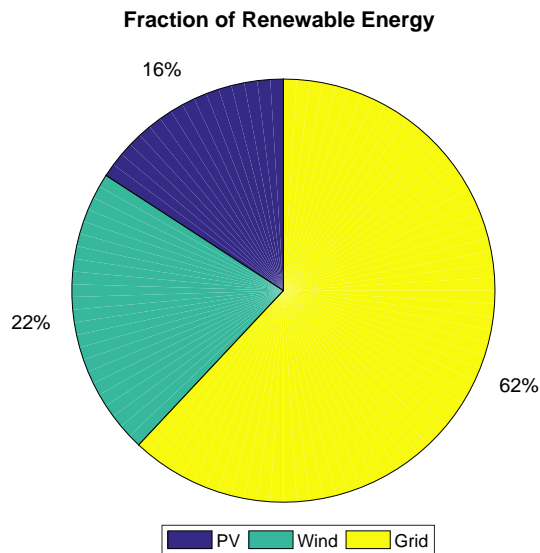


Figure 7: The contribution of PV, wind and grid in supplying the load demand, in the configuration provided by RMO.

Table 3: Comparison between the optimised and grid-only configurations over one year

configuration	PV (kWh)	Wind (kWh)	Battery (kWh)	Total Annual Cost (\$)	E_{an} (ton)
RMO	1.0e+4	1.7e+4	5.5e+3	3.7e+7	5.2e+4
Grid only	0	0	0	3.2e+7	8.4e+4

demonstrates the power dispatch for the microgrid configuration produced by RMO, over a 24-hour period. It can be observed that at 15th hour, the control and management strategy of the microgrid let the excess renewable power generation be stored in the batteries first, and if exceeds will feed in to the main grid.

6. Analysing the impact of emission-free power in the grid

Traditionally, the grid has mainly relied on power plants based on fossil fuels. Some grids include nuclear energy and increasingly, renewable energy in the mix. The proportion of renewable energy varies. As an example, in the United States, renewable energy provided 17.6% of the grid power in 2018, while about 38% of the annual energy generation was CO_2 free [41].

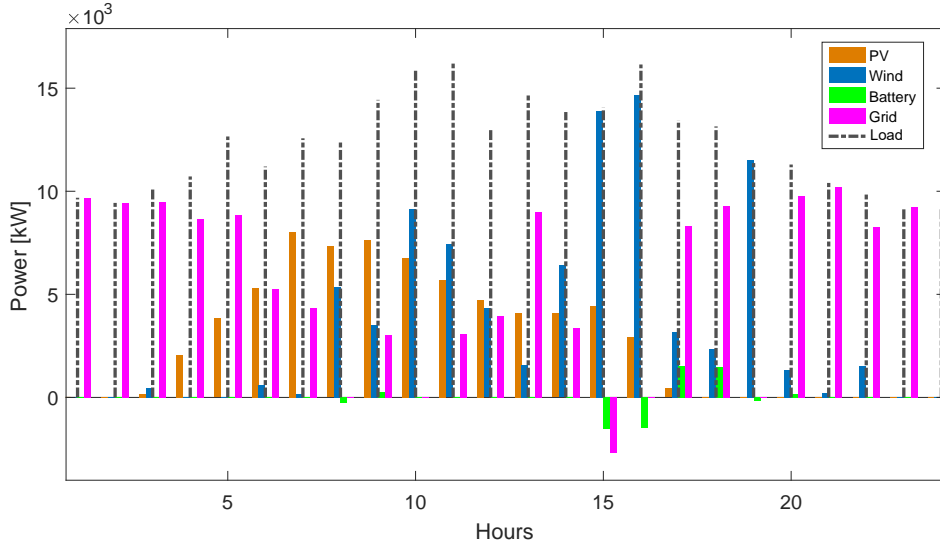


Figure 8: Power dispatch for the RMO configuration of the microgrid, over a 24-hour period.

In the simulation design explained in Section 5.3, the main grid was considered to be mainly relying on fossil fuels; therefore, greenhouse gas emissions are considered as listed in Table 1. Due to a changing climate, nations and their grid operators increasingly include renewable energy sources. Therefore, we analyse the impact of including emission-free energy generation sources such as PV systems, wind energy, nuclear power plants, and hydro-power in the main grid, on the resulting microgrid configuration.

We assume that the inclusion of emission-free power sources does not affect the electricity price. Nonetheless, for this investigation, we have used contemporary electricity pricing as experienced in Australia, listed in Table 4. Including renewable energy in the grid mix makes it necessary to adjust the emissions calculation as shown in Eq. (15).

$$E_{an} = \sum_{h=1}^{8760} \mathcal{P}_{grid}[h] \times (1 - \zeta) \times \sum_{p=1}^{\mathcal{M}} \mathcal{X}_p \quad (15)$$

In Eq. (15), ζ represents the fraction of emission-free power generation in the main grid. If ζ equals zero, the results are the same as the base scenario with all parameters as explained in Section 5.3. In contrast, if

the grid is completely emission-free, there will be no fraction of renewable energy in the microgrid configuration. We considered 11 different values for ζ and simulated the microgrid configuration for each of them individually. Fig. 9 shows the results for the contribution of renewable generation in the microgrid configuration, based on the proportion of emission-free power in the grid. As expected, by increasing ζ , the contribution of the grid increases. At ζ equals 0.9, all electricity is purchased from the main grid. There is a linear relationship between the increase in the fraction of emission-free generation in the grid, and the contribution of the grid in supplying the load demand of the microgrid.

The model assumes that the reason for installing a dedicated microgrid for a data centre is to supply the data centre with renewable energy. Installing renewable energy generation units in a microgrid is more expensive and time-consuming than purchasing electricity from the power system. Another possible reason for a microgrid is a remote location. In such cases, there usually is no chance of obtaining grid energy. Our model is obviously not suitable for such conditions. Therefore, based on the problem definition and scope of this study, if the grid is emission-free, there is no reason to include a microgrid in the solution.

7. Analysing the impact of variable electricity price on the microgrid configuration

The electricity being purchased from the grid in the base scenario is at a flat rate of 0.26 \$/kWh. However, it is not always the case, and some utility companies or main grid operators sell electricity at a variable price. The time of use (ToU) tariff is a popular pricing scheme that determines the electricity price based on the peak of community usage. It usually comprises of peak, shoulder, and off-peak periods from which peak period is when the load demand is at its highest, so as the electricity price. The off-peak period mostly covers the times that the load demand is at its lowest, e.g., usually after midnight till early morning. The remaining times is covered by shoulder period in which the electricity price is between the peak and off-peak. Table 4 shows the electricity tariff for peak, shoulder, and off-peak periods as well as the definition of each period. This pricing is obtained from the website of a typical utility company [42]. The peak period lasts for 4 hours with the electricity price of about 30% more than the flat rate used in the base

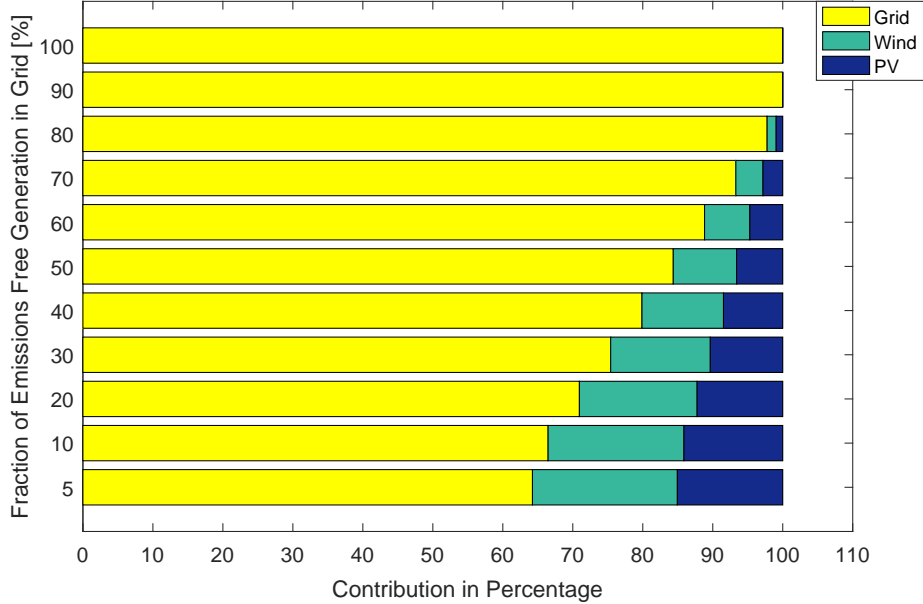


Figure 9: Impact of emission free power source inclusion in the main grid on the microgrid configuration.

scenario. In contrast, for 9 hours of each day during the off-peak period, the electricity price is about 19% less than the flat price of 0.26 \$/kWh.

Table 4: Time of use tariff for electricity purchase from the grid.

Time	Period	Price (c/kWh)
Peak	4pm to 8pm, weekdays	33.92
Shoulder	7am to 4pm, weekdays	25.44
	8pm to 10pm, weekdays	
	7am to 10pm, weekends	
off-peak	all other times	21.20

If we update the Eq. 6 with the tariff shown in Table 4, and run the simulation for the grid-only situation with no microgrid and keep all parameters as explained in Section 5.3, the total electricity cost will be $\$3.083e+7$, which is 3.8% less than purchasing the grid electricity at a flat price. In the microgrid configuration, this overall lower price of grid electricity has led to

more contribution from the main grid and less renewable energy fraction. The resultant microgrid configuration comprises of 4.1% more grid contribution on annual energy supply, compared with Fig. 7, while the contribution of wind turbines and PV panels in the annual energy supply of the microgrid is about 21% and 13% respectively.

8. Analysing the impact of trade-off factor on the optimised configuration

In order to analyse the impact of the trade-off factor, we define eight scenarios in addition to the base scenario ($\theta = 0.7$). The trade-off factor was changed from 0.1 to 0.9 and the optimisation was carried out for each scenario separately. The simulation parameters were kept constant for all simulations. The results are shown in Fig. 10. It is obvious from the figure that the higher a trade-off factor is selected, the lower the renewable energy contribution. This is due to the higher capital cost of renewable energy generation units. However, the change in the renewable fraction is not linear in the trade-off factor. The change is more dramatic when the trade-off value is closer to the constraints of 0 and 1. Almost the same pattern can be seen in Fig. 11 where the total annual cost and the total annual emissions graphs based on the trade-off factor are shown. It can be observed from the figure, that the total annual cost decreases with increasing trade-off factor, while the emissions have the opposite relationship with the trade-off factor. This is rationally conclusive, as we expect the total cost to decrease when the importance of the cost is higher in our optimisation problem.

9. Conclusions

In this paper, we presented an optimised microgrid configuration design for a green data centre. The necessity to use green energy for data centres has been recognised by larger and smaller providers. Depending on financial means, environmental conditions and local regulations, providers may be more or less ambitious in including self-generated renewables in their power supplies [16]. Technologies that optimise for different tradeoffs of renewables are therefore useful in practice. The proposed optimisation model provides such a tool, which includes mathematical models for the costs and the green gas emissions associated with all components of the microgrid system. The capital, operational, and degradation costs during a lifetime of 20 years of

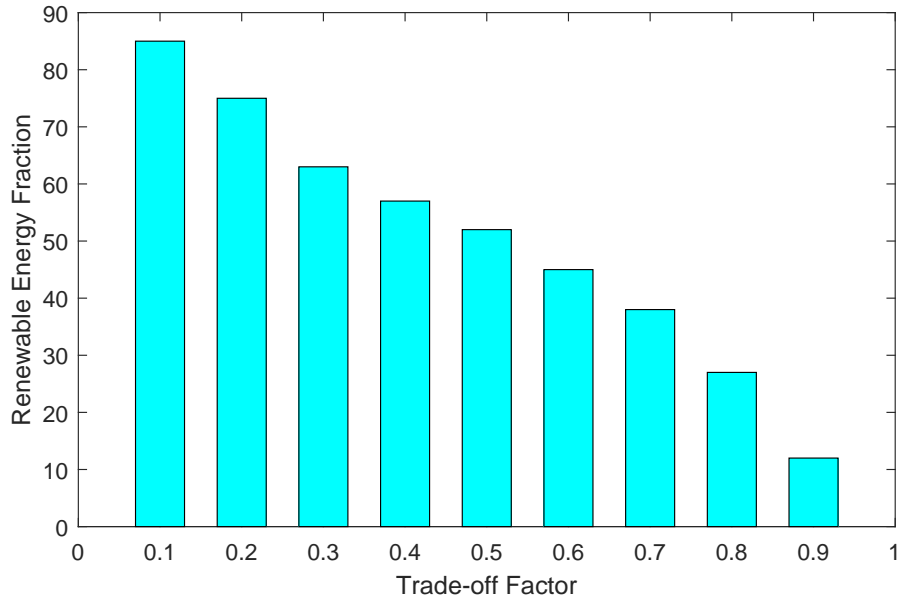


Figure 10: The optimised renewable energy fraction for different scenarios.

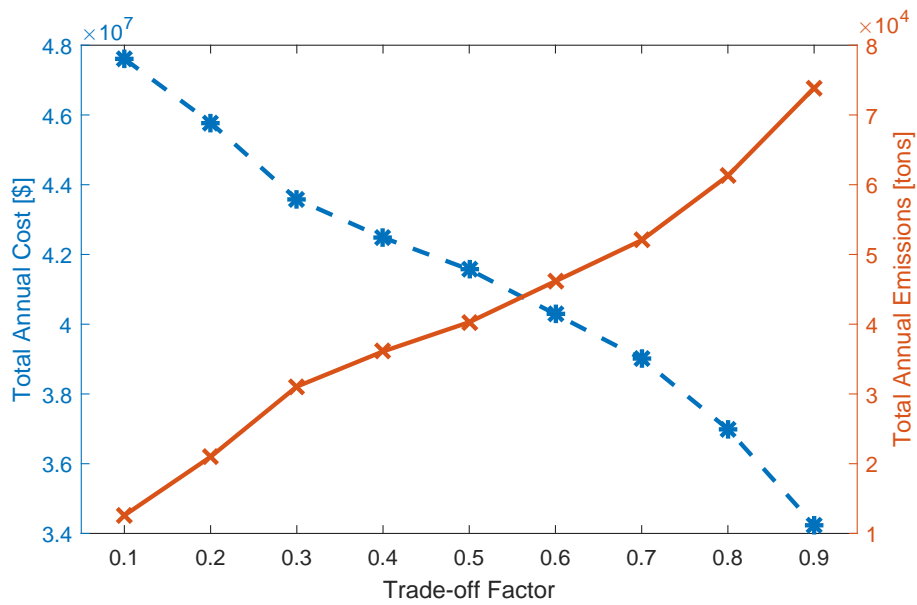


Figure 11: The change in optimised annual cost and emissions for different scenarios.

the system are also being considered. Hourly environmental data such as ambient temperature, solar irradiation and wind speed is used to calculate the renewable energy generation of the microgrid and the load demand. As a case study, a green data centre composed of 40,000 servers is modelled and its power load demand is analysed. The resulting microgrid configuration for the base scenario is composed of about 38% renewable energy generation that increases the total cost by 16.7% while the greenhouse gas emissions is reduced by 37.6%.

- [1] I. Whitfield, The importance of green data centres, <https://data-economy.com/the-importance-of-green-data-centres/>, accessed 07/01/2020.
- [2] A. López-González, B. Domenech, L. Ferrer-Martí, Sustainability and design assessment of rural hybrid microgrids in venezuela, *Energy* 159 (2018) 229–242.
- [3] E. Kabalcı, An islanded hybrid microgrid design with decentralized dc and ac subgrid controllers, *Energy* 153 (2018) 185–199.
- [4] M. Zachar, P. Daoutidis, Understanding and predicting the impact of location and load on microgrid design, *Energy* 90 (2015) 1005–1023.
- [5] T. Schütz, X. Hu, M. Fuchs, D. Müller, Optimal design of decentralized energy conversion systems for smart microgrids using decomposition methods, *Energy* 156 (2018) 250–263.
- [6] T. Cao, Y. Hwang, R. Radermacher, Development of an optimization based design framework for microgrid energy systems, *Energy* 140 (2017) 340–351.
- [7] D. Zhang, S. Evangelisti, P. Lettieri, L. G. Papageorgiou, Optimal design of chp-based microgrids: Multiobjective optimisation and life cycle assessment, *Energy* 85 (2015) 181–193.
- [8] R. Ghanaee, A. A. Foroud, Enhanced structure and optimal capacity sizing method for turbo-expander based microgrid with simultaneous recovery of cooling and electrical energy, *Energy* 170 (2019) 284–304.

- [9] E. Rosales-Asensio, M. de Simón-Martín, D. Borge-Diez, J. J. Blanes-Peiró, A. Colmenar-Santos, Microgrids with energy storage systems as a means to increase power resilience: An application to office buildings, *Energy* 172 (2019) 1005–1015.
- [10] M. Ghiasi, Detailed study, multi-objective optimization, and design of an ac-dc smart microgrid with hybrid renewable energy resources, *Energy* 169 (2019) 496–507.
- [11] H. Lotfi, A. Khodaei, Hybrid ac/dc microgrid planning, *Energy* 118 (2017) 37–46.
- [12] F. Varasteh, M. S. Nazar, A. Heidari, M. Shafie-khah, J. P. Catalão, Distributed energy resource and network expansion planning of a cchp based active microgrid considering demand response programs, *Energy* 172 (2019) 79–105.
- [13] C. Blum, J. Puchinger, G. R. Raidl, A. Roli, Hybrid metaheuristics in combinatorial optimization: A survey, *Applied Soft Computing* 11 (6) (2011) 4135–4151.
- [14] C. Blum, A. Roli, Metaheuristics in combinatorial optimization: Overview and conceptual comparison, *ACM computing surveys (CSUR)* 35 (3) (2003) 268–308.
- [15] R. Rahmani, Y. Rubiyah, N. Ismail, A new metaheuristic algorithm for global optimization over continuous search space, *ICIC Express Lett* 9 (2015) 1335–1340.
- [16] B. Gardiner, Working towards the green data centre, <https://www.cio.com/article/3492651/working-towards-the-green-data-centre.html>, accessed 07/01/2020.
- [17] S. Murugesan, Harnessing green IT: Principles and practices, *IT professional* 10 (1) (2008) 24–33.
- [18] K. Bilal, S. U. R. Malik, O. Khalid, A. Hameed, E. Alvarez, V. Wijaysekara, R. Irfan, S. Shrestha, D. Dwivedy, M. Ali, et al., A taxonomy and survey on green data center networks, *Future Generation Computer Systems* 36 (2014) 189–208.

- [19] E. Baccour, S. Fougou, R. Hamila, Z. Tari, A. Zomaya, Ptnet: An efficient and green data center network, *Journal of Parallel and Distributed Computing* 107 (2017) 3–18.
- [20] M. Ghamkhari, H. Mohsenian-Rad, Energy and performance management of green data centers: A profit maximization approach, *IEEE Transactions on Smart Grid* 4 (2) (2013) 1017–1025.
- [21] K. Ebrahimi, G. F. Jones, A. S. Fleischer, A review of data center cooling technology, operating conditions and the corresponding low-grade waste heat recovery opportunities, *Renewable and Sustainable Energy Reviews* 31 (2014) 622–638.
- [22] E. Oró, V. Depoorter, A. Garcia, J. Salom, Energy efficiency and renewable energy integration in data centres. strategies and modelling review, *Renewable and Sustainable Energy Reviews* 42 (2015) 429–445.
- [23] L. A. Barroso, J. Clidaras, U. Hölzle, The datacenter as a computer: An introduction to the design of warehouse-scale machines, *Synthesis lectures on computer architecture* 8 (3) (2013) 1–154.
- [24] T. Evans, The different technologies for cooling data centers, APC white paper 59.
- [25] W. El-Khattam, K. Bhattacharya, Y. Hegazy, M. Salama, Optimal investment planning for distributed generation in a competitive electricity market, *IEEE Transactions on power systems* 19 (3) (2004) 1674–1684.
- [26] R. C. Dugan, T. E. McDermott, G. J. Ball, Planning for distributed generation, *IEEE industry applications magazine* 7 (2) (2001) 80–88.
- [27] X. Tang, G. Tang, Multi-objective planning for distributed generation in distribution network, in: *Electric Utility Deregulation and Restructuring and Power Technologies, 2008. DRPT 2008. Third International Conference on*, IEEE, 2008, pp. 2664–2667.
- [28] E. Ingram, Building on hydros strengths to integrate solar, microgrid into a portfolio, <https://www.renewableenergyworld.com/2019/11/20/building-on-hydros-strengths-to-integrate-solar-microgrid-into-a-portfolio/>, accessed 07/01/2020.

- [29] T. Logenthiran, D. Srinivasan, Optimal selection and sizing of distributed energy resources for distributed power systems, *Journal of Renewable and Sustainable Energy* 4 (5) (2012) 053119.
- [30] J. Stultz, L. Wen, Thermal performance testing and analysis of photovoltaic modules in natural sunlight, LSA Task Report 5101 (1977) 31.
- [31] R. Rahmani, A. Khairuddin, S. M. Cherati, H. M. Pesaran, A novel method for optimal placing wind turbines in a wind farm using particle swarm optimization (pso), in: *IPEC, 2010 Conference Proceedings*, IEEE, 2010, pp. 134–139.
- [32] C. Zou, A. G. Kallapur, C. Manzie, D. Nešić, Pde battery model simplification for soc and soh estimator design, in: *Decision and Control (CDC), 2015 IEEE 54th Annual Conference on*, IEEE, 2015, pp. 1328–1333.
- [33] S. K. Kollimalla, A. Ukil, H. Gooi, U. Manandhar, N. R. Tummuru, Optimization of charge/discharge rates of a battery using a two-stage rate-limit control, *IEEE Transactions on Sustainable Energy* 8 (2) (2017) 516–529.
- [34] V. Prajapati, H. Hess, E. J. William, V. Gupta, M. Huff, M. Manic, F. Rufus, A. Thakker, J. Govar, A literature review of state-of-charge estimation techniques applicable to lithium poly-carbon monofluoride (li/cfx) battery, in: *Power Electronics (IICPE), 2010 India International Conference on*, IEEE, 2011, pp. 1–8.
- [35] K. Rahbar, J. Xu, R. Zhang, Real-time energy storage management for renewable integration in microgrid: An off-line optimization approach, *IEEE Transactions on Smart Grid* 6 (1) (2015) 124–134.
- [36] H. Delavaripour, H. R. Karshenas, A. Bakhshai, P. Jain, Optimum battery size selection in standalone renewable energy systems, in: *Telecommunications Energy Conference (INTELEC), 2011 IEEE 33rd International*, IEEE, 2011, pp. 1–7.
- [37] S. Mizani, A. Yazdani, Optimal design and operation of a grid-connected microgrid, in: *Electrical Power & Energy Conference (EPEC), 2009 IEEE*, IEEE, 2009, pp. 1–6.

- [38] R. Rahmani, R. Yusof, A new simple, fast and efficient algorithm for global optimization over continuous search-space problems: Radial movement optimization, *Applied Mathematics and Computation* 248 (2014) 287–300.
- [39] M. Macías, J. Guitart, SLA negotiation and enforcement policies for revenue maximization and client classification in cloud providers, *Future Generation Computer Systems* 41 (2014) 19–31.
- [40] R. Rahmani, I. Moser, M. Seyedmahmoudian, A complete model for modular simulation of data centre power load, arXiv preprint arXiv:1804.00703.
- [41] C. Marcy, U.s. renewable electricity generation has doubled since 2008, U.S. Energy Information Administration March, 19.
- [42] Clickenergy energy price fact sheet - click shine electricity tariff,, *online*,, accessed: 2017-05-30.